# Hole Transfer from Low Bandgap Quantum Dots to Conjugated Polymers in Organic/Inorganic Hybrid Photovoltaics

*Adam E. Colbert*[†], *Eric M. Janke*[†], *Stephen T. Hsieh*[†], *Selvam Subramaniyan*[‡], *Cody W. Schlenker*[†], *Samson A. Jenekhe*[‡], *and David S. Ginger**[,†]

[†] Department of Chemistry, University of Washington, Box 351700, Seattle, Washington 98195-1700

[‡] Department of Chemical Engineering, University of Washington, Box 351750, Seattle, Washington 98195-1750

Email: Email: ginger@chem.washington.edu

## Section S1) Experimental Methods

*PbS Nanocrystal Synthesis and Halide Treatment*

Colloidal PbS QDs were synthesized using a modified procedure described by Hines and Scholes.[1] Surface passivation by a partial oleate-to-iodide ligand exchange was performed *in-situ* based on the work of Ning *et al*.[2] The lead precursor was prepared by mixing PbO (0.45 g, 2.00 mmol), oleic acid (1.6 g, ~5.6 mmol), and 1-octadecene (ODE) (14 g) in a three-neck flask and stirring under vacuum at 105° C for at least 1 hr. After the solution turned clear, the flask was placed under nitrogen flow and the temperature was increased to 165° C. Meanwhile, iodide and sulfur precursors were prepared in separate three-neck flasks. For the iodide precursor, oleylamine (0.8 g) and tetrabutylammonium iodide (TBAI) (200 mg) were added to a 25 ml flask

3-neck flask and degassed under vacuum. While stirring under vacuum, the iodide precursor was heated to 200° C for 1 hr. Subsequently, the temperature was reduced to 50° C, vacuum was ceased and the flask remained under nitrogen flow. The sulfur precursor was prepared in a separate three-neck flask by addition of 210 μL (1 mmol) Hexamethyldisilathiane (HMDS) to 4 g of ODE under nitrogen gas flow. The sulfur precursor was rapidly injected into the hot lead precursor solution. Upon injection, heat to the reaction flask was immediately switched off and the mixture was left on the heating mantle to slowly cool.

Once the temperature of the reaction solution reached 70° C, ~0.75 mL of the contents of the iodide precursor flask was injected into the PbS colloid flask and stirred under flow of nitrogen for 20 min. The quantum dot product was isolated from the unreacted precursors by precipitation with acetone followed by centrifugation. The product was cleaned in ambient air by dissolving the precipitate in a minimal volume of hexanes and precipitating once with acetone and twice with methanol. The final product was dried under nitrogen and transferred to a glovebox where it was dissolved in anhydrous chlorobenzene.

*ZnO Nanocrystal Synthesis*

Colloidal ZnO nanocrystals were prepared in ambient atmosphere using an adaptation of procedures described elsewhere.[3-5] Briefly, zinc acetate dihydrate (5.25 g, 24 mmol) was dissolved in 200 ml methanol by stirring at 60° C and subsequently reacted via dropwise addition of 100 mL of 0.4 M KOH in methanol. The mixture was stirred under mild refluxing conditions for 2 hr. The resulting opaque white colloid was isolated from unreacted precursors by centrifugation at 1200 rpm. The isolated nanocrystals were cleaned 3 times by addition of 10 mL methanol, agitation by vortexing, and centrifugation. The supernatant was discarded between

cycles. Finally, the ZnO nanocrystals were dispersed in chloroform at a concentration of ~80 mg/mL.

*PDTPQx-HD Synthesis*

Poly(2,3-bis(2-(hexyldecyl)-quinoxaline-5,8-diyl-*alt*-N-(2-hexyldecyl)-dithieno[3,2-b:2′,3′-d]pyrrole) (PDTPQx-HD) was synthesized as reported previously.[6] The polymer structure is shown below in Figure S1.

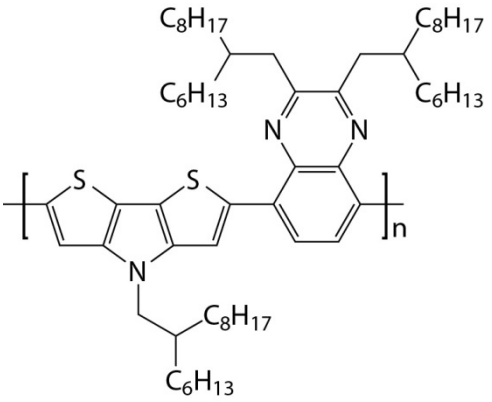


**Figure S1**. Chemical structure of PDTPQx-HD.

*Device and PIA Sample Fabricaton*

Pre-etched 1.5 $cm^2$ substrates of indium tin oxide (ITO) coated were cleaned by sonication in acetone followed by isopropanol for 30 min. each. ITO substrates were then cleaned by air plasma treatment for 10 minutes. ZnO was immediately spin-cast from a chloroform solution at 2500 rpm to give a ~65 nm coating of ZnO nanocrystals (as measured by profilometry). Coated substrates were then annealed at 250° C for 30 minutes in air, then cooled to room temperature. All subsequent sample preparation steps were performed in a nitrogen glovebox. A 20 mg/mL solution of PDTPQx-HD was prepared in anhydrous chlorobenzene and stirred at 50° C for at least 4 hr. A blend solution was prepared by mixing the PbS and PDTPQx-HD solutions in a 1:9

(w/w) ratio, and stirring at 50° C for at least 4 hr. PDTPQx-HD/PbS active layers were then spin-cast on ZnO coated ITO by a 2 seconds at 1200 rpm followed by 1 minute at 1800 rpm. PDTPQx-HD/PCBM blends were prepared in a similar manner by mixing the PDTPQx-HD solution with a 40 mg/mL solution of $PC_{61}BM$ in chlorobenzene in a 1:1 (w/w) ratio. For PIA samples, films were spin cast under the same conditions onto glass microscope slides. Spin-cast films were treated with 3-mercaptopropionic (MPA) to remove insulating oleate ligands and passivate the surface according to a procedure adapted from the literature.[7,8] Films were treated with a 1 mmol solution of MPA in anhydrous methanol three times by coating the film surface with the solution, waiting for 1 minute, then blowing the film dry with a stream of nitrogen. The films were subsequently washed with anhydrous methanol and blown dry three times to remove residual quantum dot ligand. Photovoltaic device back contacts of $MoO_3$ (10 nm)/Ag (100 nm) were and were deposited by consecutive thermal evaporations from a base pressure of less than $5\times10^{-7}$ torr. Individual pixels were defined by a shadow mask.

*Photovoltaic Device Measurements*

Photocurrent spectra were obtained with a monochromated tungsten-halogen lamp and measured with a Keithley 2400 source measure unit. External quantum efficiency (EQE) values were calculated using calibrated silicon (OSI optoelectronics) and indium gallium arsenide (Thorlabs) photodiodes. The calibrated photodiodes and the device pixels were masked with identical 1.22 $mm^2$ active areas. The devices were held under active vacuum during device testing.

*Photoinduced Absorption Measurements*

PIA and frequency-dependence measurements were acquired using standard lock-in techniques detailed elsewhere.[9,10] The 2.77 eV (447 nm) excitation source was a light-emitting diode (LED; Luxeon Rebel, 700 mW, LXML-PR01-0425) equipped with a 550 nm long pass filter to block pump light from entering the detector. The 1.97 eV (630 nm) pump was an LED (Luxeon Rebel, 700 mW, LXM2-PD01-0040) equipped with a 700 nm long pass filter. Both LEDs were powered with a home-built driver circuit. The LEDs were modulated by an Agilent 33120A arbitrary waveform generator. The 1.27 eV (975 nm) excitation source was a 1000 mW laser diode (ThorLabs L975P1WJ), modulated with an optical chopper (Stanford Research Systems SR540). Quasi-steady-state measurements were conducted with a pump modulation frequency of 200 Hz. The probe beam was a monochromated 100 W tungsten halogen lamp and was monitored with with a Si/InGaAs dual-band photodetector (ThorLabs, DSD2) with sensitivity ranging from 500-1700 nm in the case of quasi-steady-state measurements, or an amplified Si photodiode (ThorLabs PDA36A) with sensitivity up to 1100 nm in the case of frequency-dependence measurements. At each measured probe energy, fractional changes in probe beam transmission ($\Delta T$) were detected with a Stanford Research Systems SR830 lock-in amplifier which were normalized to the probe beam transmission ($T$), and corrected for sample photoluminescence by recording data with the probe beam blocked. Values are reported as normalized negative differential transmission ($-\Delta T/T$). The phase of the lock-in was set using reflected pump light such that the signal was entirely in the positive X-channel (in-phase). The Y-channel (quadrature) detector is 90° phase lagged from the X-channel. Samples were held under active vacuum during PIA measurements.

## Section S2). Absorbance of PDTPQx-HD/$PC_{61}BM$

Supporting Information Figure S2 shows the thin film absorbance of the PIA sample used to obtain the data in Figure 3a of the text. The sample shows no absorbance for energies lower than ~1.4 eV, resulting in the lack of signal in the PIA spectrum for this sample when excited at 1.27 eV.

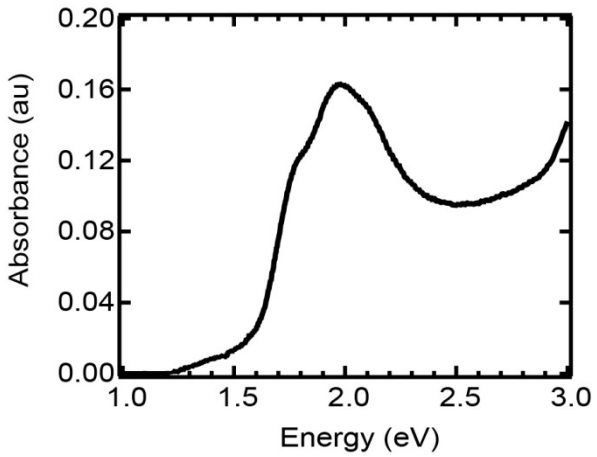


**Figure S2**. PDTPQx-HD/$PC_{61}BM$ thin film absorbance spectrum. The sample consisted of a 1:1 (w/w) ratio bulk heterojunction blend of PDTPQx-HD/$PC_{61}BM$.

## Section S3) Modulation Dependence of Polaron and EA Photoinduced Absorption Features

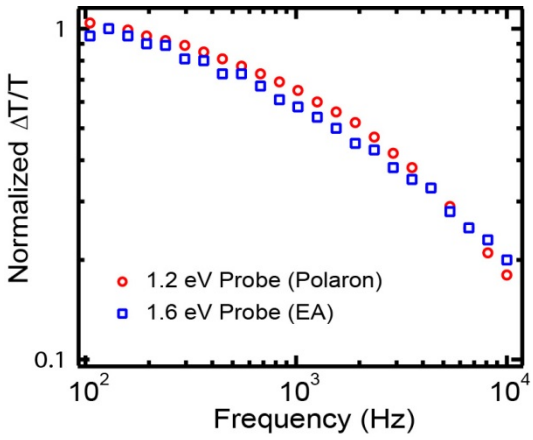

**Figure S3**. Pump modulation dependence of the 1.2 (red circles) and 1.6 eV (blue squares) PIA spectral features of a PDTPQx-HD/PCBM blend under 2.77 eV excitation.

## Section S4). Unnormalized In-Phase and Quadrature PIA Spectra of PDTPQx-HD/PbS

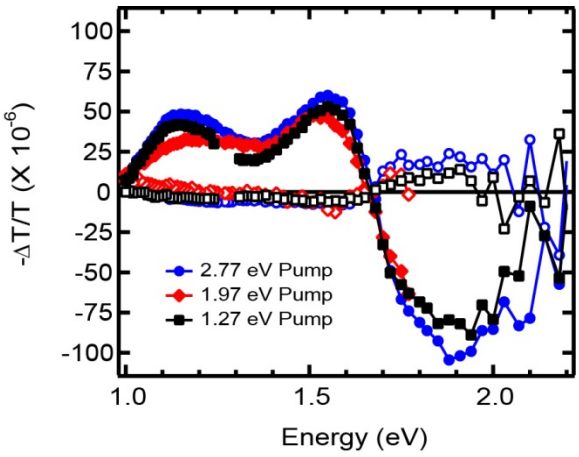


**Figure S4**. Unnormalized PIA spectra of the hybrid-passivated PDTPQx-HD/PbS film from Figure 3b in the main text, acquired under 2.77 (blue circles), 1.97 (red diamonds), and 1.27 eV (black squares) excitation. Filled symbols correspond to X-channel (in-phase) signal and hollow symbols represent Y-channel (quadrature) signal. No significant changes in lineshape or the ratio of X-channel to Y-channel signal occur between the different excitation energies.

## Section S5) Thiol Treatment of PDTPQx-HD/PCBM and neat PDTPQx-HD: No Significant Changes in PIA Spectra

To ensure that the post-deposition 3-mercaptopropionic acid (MPA) treatment of the PDTPQx-HD/PbS samples did not cause significant morphological changes or chemical doping of the polymer phase, we tested the effects of treating PDTPQx-HD/PCBM and neat PDTPQx-HD films with a 1 mM solution of MPA in anhydrous methanol. Figure S5a shows that the PIA

spectrum of PDTPQ-HD/PCBM is not affected by the thiol treatment. Accordingly, modulation dependence of the polaron feature shown in Figure S5b shows no significant differences in recombination lifetime resulting from MPA treatment. Furthermore, the neat polymer also shows no effects from the thiol treatment in the PIA and absorbance spectra as shown in Figure S5c and S5d, respectively.

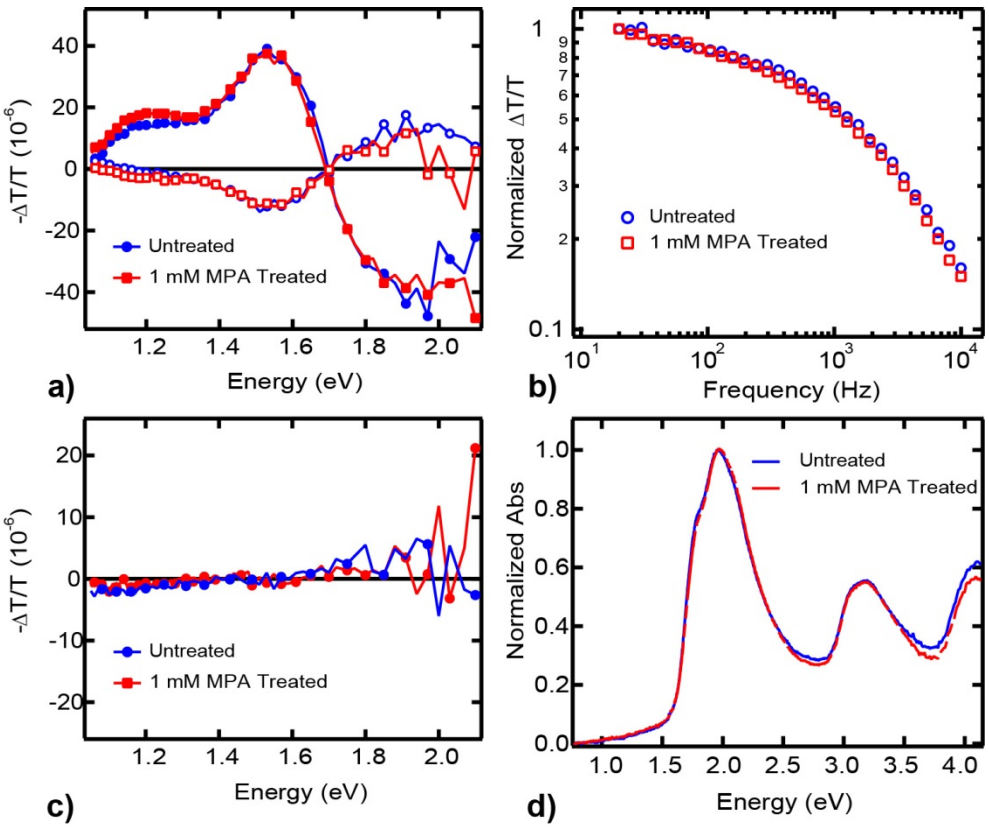


**Figure S5.** (a) PIA spectra of PDTPQx-HD/PCBM before (blue circles) and after (red squares) MPA-treatment. Filled symbols represent the X-channel (in-phase) portion of the data, and unfilled symbols represent the Y-channel (quadrature) portion of the data. (b) Modulation dependence of PDTPQx-HD/PCBM before (blue circles) and after (red squares) MPA-treatment. (c) X-Channel PIA and (d) absorbance spectra of neat PDTPQx-HD before (blue lines) and after (red lines) MPA-treatment. All PIA spectra were acquired under 2.77 eV excitation.

## Section S6) Photoinduced Absorption of Neat PbS

Figure S6 compares the PIA spectra of a neat (solution TBAI-treated) PbS quantum dot film before (blue diamonds) and after (red circles) post-deposition treatment with 1 mM MPA against the PIA spectrum of hybrid-passivated PDTPQx-HD/PbS. A weak bleach feature can be seen at the optical band gap of the quantum dots (~1.07 eV), corresponding to a bleach of the first excitonic transition ($^1S_h$ to $^1S_e$). The magnitude of the signal is seen to increase slightly following MPA treatment. The quantum dot bleach overlaps the shoulder of the PDTPQx-HD polaron transition, and is therefore hidden in the polymer/quantum dot blend PIA spectrum.

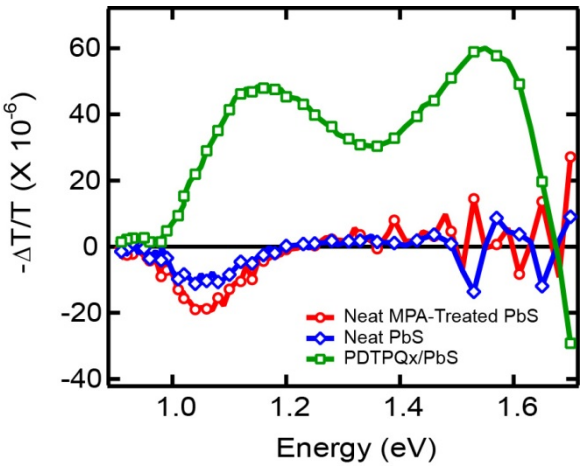


**Figure S6**. X-channel PIA spectra of a neat (solution TBAI-treated) PbS quantum dot film before (blue diamonds) and after (red circles) MPA-treatment, and hybrid-passivated PDTPQx-HD/PbS (green squares) under 2.77 eV excitation.

## Section S7) Determining Polaron Lifetimes from PIA Pump Modulation Dependence

The dependence of PIA signal on pump modulation frequency can be used to determine an average polaron lifetime fit parameter. Figure S6 displays traces for the three different pumps (2.77, 1.97, and 1.27 eV), fit using the dispersive recombination equation[6,11] shown in the figure inset. The dispersive fit parameters are nearly identical for the three different curves, with nearly identical lifetime distribution fitting parameters of $\tau \approx 0.25$ ms, and dispersion parameters of $\gamma \approx 0.67$.

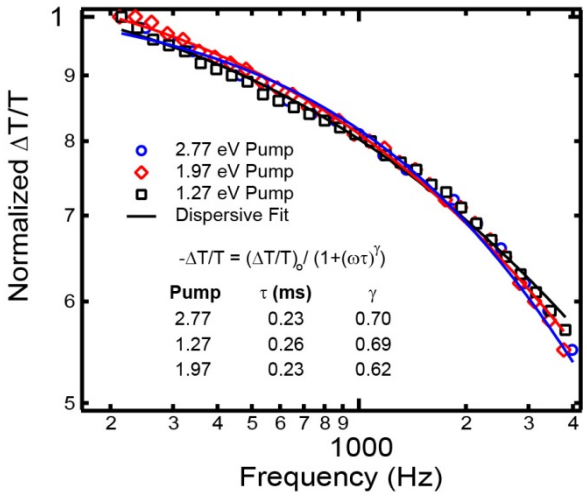


**Figure S7**. Modulation frequency dependence of the PIA signal (ΔT/T) monitored at the 1.85 eV polaron transition with varying pumps: 2.77 (blue circles), 1.97 (red diamonds), and 1.27 eV (black squares). Fit parameters ($\tau$ and $\gamma$) were determined by dispersive fits of the data to the inset model (solid lines) as a function of modulation frequency $f = \omega/(2\pi)$.

## Section S8) Calculation of Quantum Dot and Polymer Polaron Yields

Figure S8a shows the dependence of the polaron PIA signal magnitude, R ($=(X^2 + Y^2)^{1/2}$), on absorbed pump flux for hybrid-passivated PDTPQx-HD/PbS with 1.27 and 1.97 eV excitation. The relative pump power at each point was determined by measuring the photocurrent of a

calibrated silicon photodiode through an aperture cut to the *probe* spot size. The pump spot size was larger than the probe spot size, and therefore, only the portion of the pump spot overlapping the probe beam was measured. The relative flux (photons/s) was then calculated using the calibrated diode's spectral responsivity and the known pump photon energy. The total absorbed photons per second ($\Phi_{Abs}$) for each pump intensity was subsequently determined based on the photon flux and the film optical density at the corresponding excitation wavelength.

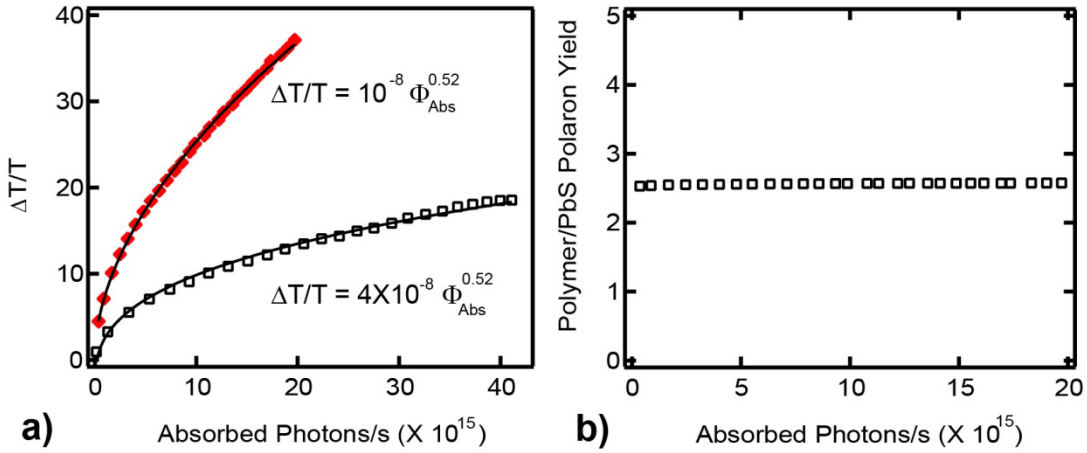


**Figure S8**. (a) Dependence of the PIA signal on absorbed pump photon flux ($\Phi_{Abs}$) for the PDTPQx/PbS polaron transition under 1.97 (red diamonds) and 1.27 eV (black squares) excitation. The data were fit with power law curves (solid lines), with the fit equations inset under the respective curves. (b) Calculated ratio of polaron yields from polymer and quantum dot light absorption under 1.97 eV excitation at varying excitation densities.

Figure S8b shows that the calculated ratio of polaron yields (ΔT/T per photons/s absorbed) generated from polymer and quantum dot components remains constant with changing excitation intensity. The 1.27 eV pump data was interpolated at each measured value of the 1.97 eV pump to compare the ΔT/T values for the two different pumps *with the same number of absorbed*

*photons*. Figure S9 shows the absorbance spectra of the quantum dots and polymer/quantum dot blend (in solution), normalized to the quantum dot exciton peak. The difference between the two spectra was used to determine the fraction of photons from the 1.97 eV pump absorbed by the quantum dot species. As discussed in the text, we assume that the observed polaron yield is independent of the excitation wavelength. Since the polaron signal generated by 1.27 eV excitation originates only from quantum dot absorption, we used the interpolated 1.27 eV pump data and the percentage of quantum dot light absorption at 1.97 eV to calculate the expected quantum dot polaron yield under 1.97 eV illumination (for small values of ΔT/T, ΔT/T is directly proportional to the absorbance). The polymer polaron yield was then determined using the difference between the total PIA signal and the calculated quantum dot polaron yield.

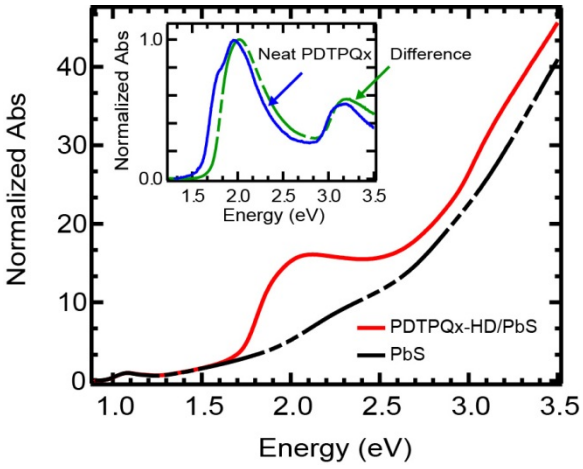


**Figure S9.** Absorbance spectra of the PDTPQx-HD/PbS blend solution (used to fabricate films for device and PIA data) (red line) and the PbS quantum dots (dashed black line) in tetrachloroethylene, normalized to the quantum dot exciton peak. The inset compares the normalized absorbance of a neat PDTPQx-HD film (blue line) to the difference spectrum of the blend and quantum dots (dashed green line).

## Section S9) Driving Force for Electron and Hole Transfer

We determined the driving force for photoinduced electron transfer using the excited state ionization energy (the potential necessary to oxidize the photoexcited material) of the polymer donor species as described in the literatue.[12] We calculate the polymer excited state ionization energy ($IE_{(M+/M^*)}$) from the ground state ionization energy ($IE_{(M+/M)}$) and the singlet exciton energy $E_g^{Opt}$ according to Equation 1 below.

$$IE_{(M+/M^*)} = IE_{(M+/M)} + E_g^{Opt} \quad (1)$$

This approximation accounts for the binding energy of the exciton, considering the driving force for charge separation ($\Delta E_{elec}$) in terms of exciton dissociation to a ground-state acceptor, according to Equation 2.

$$\Delta E_{elec} = EA_{(M/M-)}\,[\text{Acceptor}] - IE_{(M+/M^*)}\,[\text{Donor}] \quad (2)$$

This approximation is not used for the hole transfer process due to the low exciton binding energy of the inorganic nanocrystals. In this case, the driving force for charge separation ($\Delta E_{hole}$) was approximated by the energy difference of the polymer and quantum dot ground state ionization energies. Figure S10 shows the estimated energies for determining the driving force of photoinduced charge separation. We calculate the driving forces for electron and hole transfer to be -0.52 and -0.27 eV, respectively.

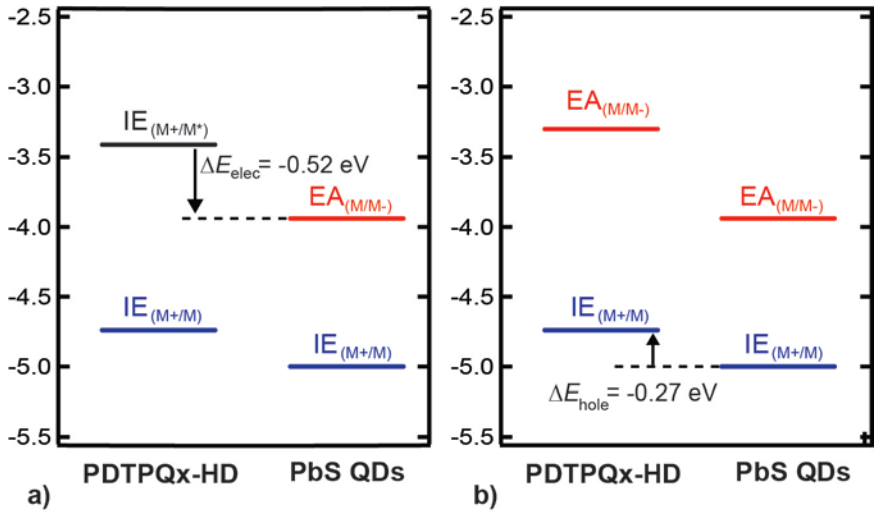


**Figure S10**. Energy levels for calculating the driving force for photoinduced (a) electron transfer and (b) hole transfer in hybrid-passivated PDTPQx-HD/PbS composites. The black line indicates the donor excited state ionization energy ($IE_{(M+/M^*)}$), blue lines represent ground state ionization energies ($IE_{(M+/M)}$), and red lines show ground state electron affinities ($EA_{(M/M-)}$).

## References

(1) Hines, M. A.; Scholes, G. D. Colloidal PbS Nanocrystals With Size-Tunable Near-Infrared Emission: Observation of Post-Synthesis Self-Narrowing of the Particle Size Distribution. *Adv. Mater.* **2003,** *15*, 1844-1849.

(2) Ning, Z.; Ren, Y.; Hoogland, S.; Voznyy, O.; Levina, L.; Stadler, P.; Lan, X.; Zhitomirsky, D.; Sargent, E. H. All-Inorganic Colloidal Quantum Dot Photovoltaics Employing Solution-Phase Halide Passivation. *Adv. Mater.* **2012**, *24*, 6295-6299.

(3) Pacholski, C.; Kornowski, A.; Weller, H. Self-Assembly of ZnO: From Nanodots to Nanorods. *Angew. Chem. Int. Edit.* **2002,** *41*, 1188-1191.

(4) Beek, W. J. E.; Wienk, M. M.; Kemerink, M.; Yang, X.; Janssen, R. A. J. Hybrid Zinc Oxide Conjugated Polymer Bulk Heterojunction Solar Cells. *J. Phys. Chem. B* **2005,** *109*, 9505-9516.

(5) Gao, J.; Perkins, C. L.; Luther, J. M.; Hanna, M. C.; Chen, H.-Y.; Semonin, O. E.; Nozik, A. J.; Ellingson, R. J.; Beard, M. C. n-Type Transition Metal Oxide as a Hole Extraction Layer in PbS Quantum Dot Solar Cells. *Nano Lett.* **2011,** *11*, 3263-3266.

(6) Noone, K. M.; Subramaniyan, S.; Zhang, Q.; Cao, G. Z.; Jenekhe, S. A.; Ginger, D. S. Photoinduced Charge Transfer and Polaron Dynamics in Polymer and Hybrid Photovoltaic Thin Films: Organic vs Inorganic Acceptors. *J. Phys. Chem. C* **2011,** *115*, 24403-24410.

(7) Pattantyus-Abraham, A. G.; Kramer, I. J.; Barkhouse, A. R.; Wang, X.; Konstantatos, G.; Debnath, R.; Levina, L.; Raabe, I.; Nazeeruddin, M. K.; Grätzel, M.; Sargent, E. H. Depleted-Heterojunction Colloidal Quantum Dot Solar Cells. *ACS Nano* **2010,** *4*, 3374-3380.

(8) Ip, A. H.; Thon, S. M.; Hoogland, S.; Voznyy, O.; Zhitomirsky, D.; Debnath, R.; Levina, L.; Rollny, L. R.; Carey, G. H.; Fischer, A.; Kemp, K. W.; Kramer, I. J.; Ning, Z. J.; Labelle, A. J.; Chou, K. W.; Amassian, A.; Sargent, E. H. Hybrid Passivated Colloidal Quantum Dot Solids. *Nat. Nanotechnol.* **2012,** *7*, 577-582.

(9) Ginger, D. S.; Greenham, N. C. Photoinduced Electron Transfer From Conjugated Polymers to CdSe Nanocrystals. *Phys. Rev. B* **1999,** *59*, 10622-10629.

(10) Noone, K. M.; Anderson, N. C.; Horwitz, N. E.; Munro, A. M.; Kulkarni, A. P.; Ginger, D. S. Absence of Photoinduced Charge Transfer in Blends of PbSe Quantum Dots and Conjugated Polymers. *ACS Nano* **2009,** *3*, 1345-1352.

(11) Heinemann, M. D.; von Maydell, K.; Zutz, F.; Kolny-Olesiak, J.; Borchert, H.; Riedel, I.; Parisi, J. Photo-induced Charge Transfer and Relaxation of Persistent Charge Carriers in Polymer/Nanocrystal Composites for Applications in Hybrid Solar Cells. *Adv. Funct. Mater.* **2009,** *19*, 3788-3795.

(12) Ren, G.; Schlenker, C. W.; Ahmed, E.; Subramaniyan, S.; Olthof, S.; Kahn, A.; Ginger, D. S.; Jenekhe, S. A. Photoinduced Hole Transfer Becomes Suppressed with Diminished Driving Force in Polymer-Fullerene Solar Cells While Electron Transfer Remains Active. *Adv. Funct. Mater.* **2012**, DOI: 10.1002/adfm.201201470.